Optical, mechanical and dielectric studies on bis (4-nitrophenol) - 2,4,6 -triamino 1, 3, 5- triazine monohydrate

N. KANAGATHARA[a], M. K. MARCHEWKA[b], S. GUNASEKARAN[c], G. ANBALAGAN[d*]
[a] *Department of Physics, Vel Tech University, Avadi, Chennai-62, India.*
[b] *Institute of Low Temperature and Structure Research, Polish Academy of Sciences, 50-950 Wrocław, 2, P.O. Box 937, Poland*
[c] *St. Peter's University, Avadi, Chennai-54*
[d] *Department of Physics, Presidency College, Chennai-5, India*

A new organic-organic salt, bis (4-nitrophenol) 2, 4, 6 -triamino 1, 3, 5- triazine monohydrate (BNPM) has been synthesized by slow evaporation technique at room temperature. X-ray powder diffraction studies confirm the crystalline nature of the grown crystals. The UV-Vis spectrum of BNPM shows less optical absorption in the entire visible region. Mechanical strength and its related parameters of BNPM have been determined by Vickers micro hardness test. The dielectric response of BNPM was studied in the frequency range 50Hz to 5 MHz at different temperatures and the results are discussed. DSC measurements on powder sample indicate the phase transition point at 366 and 306 K for heating and cooling respectively. No detectable signal was observed during powder test for second harmonic generation.

(Received October 20, 2013; accepted November 13, 2014)

Keywords: X-ray powder diffraction, Optical studies, Dielectric studies, Mechanical studies

1. Introduction

Semi organic crystals are generally believed to satisfy the material demands in electronic industry. Hence in the recent years researchers are showing their attention towards the development of new semi organic crystals for the device fabrication. Melamine (2,4,6-triamino 1,3,5–triazine), a crystalline N-heterocyclic organic base is an industrial chemical intermediate product, mainly used to manufacture plastics, dyes, fertilizers and fabrics [1]. Melamine molecule could be used as an organic part of investigated crystals. This molecule and its polymers found application in a wide variety of technological fields [2]. Melamine and its derivatives have wide applications in industry as a fire retardant substance. The use of melamine resin in automobile paints was examined by Zieba-Palus [3]. P-nitrophenol derivatives are interesting candidates as they are a typical one dimensional donor-acceptor π system, and the presence of phenolic –OH favours the formation of salts with various organic and inorganic bases. Both melamine and p-nitrophenol has wide applications in industry. A lot of theoretical works were performed to explain the behaviour of melamine molecule in the solid state [4–10]. The crystal structure of bis (4-nitrophenol) 2, 4, 6 -triamino 1, 3, 5- triazine monohydrate (BNPM) was reported by Kanagathara *et al* [11]. Vibrational spectral and density functional studies of BNPM were also studied [12]. In this work, we report the optical, mechanical, dielectric and phase transition behavior of BNPM in detail.

2. Materials and methods

High purity AR grade samples of melamine (Merck 99%) and p-nitrophenol (Sigma Aldrich) were taken in 1:1 molar ratio. At first, melamine was dissolved in double distilled water and the solution was slightly heated to a temperature of 60°C for 20-30 minutes. To the hot solution of melamine, the dissolved p-nitrophenol solution was added gently, and stirred continuously well for 5 hours to get the homogenous solution. Then the solution was filtered and allowed to evaporate at room temperature, which yielded yellowish crystals within a period of 25-30 days. The photograph of as-grown single crystal of BNPM is shown in Fig. 1 and the reaction scheme is given below

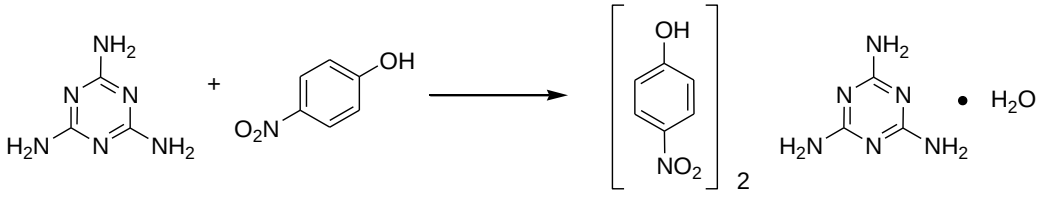

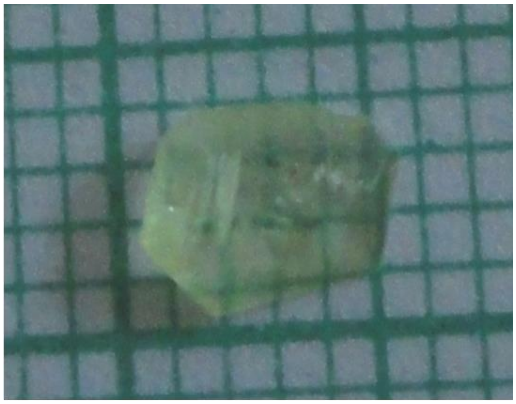

Fig. 1. Photograph of BNPM crystal.

3. Characterization

X-ray powder diffraction data of BNPM crystal were collected at room temperature using Rich Seifert X-ray powder Diffractometer with CuK_α radiation (λ=1.5406 Å) in the 2θ range from 10 - 70º at a scanning rate of 1º min^{-1} for the finely crushed powder. From the X-ray data, the various planes of reflections were indexed using XRDA 3.1 program and the lattice parameters were evaluated. The UV-Vis spectrum of BNPM was recorded between 200-800 nm using CARY/5E/UV (Arithmetic model) spectrophotometer. Micro hardness measurements were made using a Leitz micro hardness tester fitted with diamond pyramidal indenter. Suitably cut and polished section of BNPM was subjected to dielectric studies using a HIOKI model 3532-50 LCR HITESTER with a conventional two terminal sample holder. The sample was electrode on either side with air-drying silver paste so that it behaves like a parallel capacitor. The studies were carried out from 313K to 373 K for frequency varying from 50Hz to 5 MHz. DSC was carried out on NETZSCH DSC 204 analyzer with an initial mass of 3.850 mg in the temperature range 0-120°C. The grown crystals BNPM was subjected to Kurtz second harmonic generation test by using Nd:YAG Q switched laser beam with input pulse of 0.68 J for the non linear optical property.

4. Results and discussion

4.1. X-ray Powder diffraction analysis

Fig. 2 shows the indexed X-ray powder diffraction pattern of BNPM. From the X-ray powder diffraction data, the lattice parameters and the unit cell volume have been calculated and the obtained crystallographic data are a=7.167±0.070Å, b=10.242±0.040Å, c=13.055±0.2244 Å, α=72.29±0.29°, β=88.72±0.46°, γ=74.80±0.27° and V=879.20 $(Å)^3$. The data reveal a close agreement with the reported value [11].

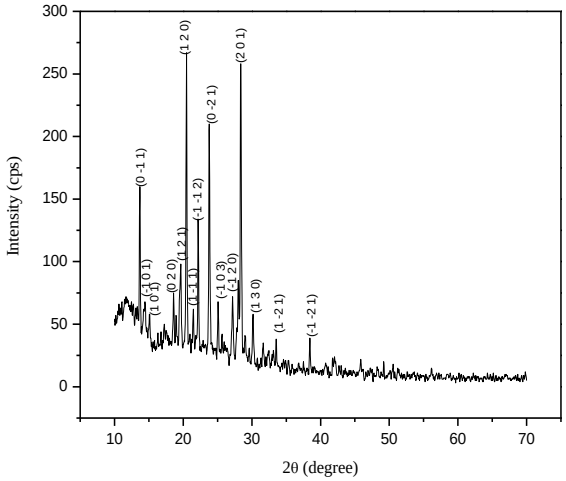

Fig. 2. Indexed X-ray powder diffraction pattern of BNPM.

4.2. Determination of some characteristic data

Molecular formula: $(2C_6H_5NO_3.\ C_3H_6N_6.H_2O)$

The crystals obtained are crystallizes in triclinic system with centrosymmetric space group P-1. The theoretical calculations show that the high frequency dielectric constant is explicitly dependent on the valence electron plasma energy, Penn gap and Fermi energy. The Penn gap is determined by fitting the dielectric constant with the plasma energy [13]. The valance electron plasma energy is given by [14]

$$\hbar\omega_p = 28.8(Z\rho / M)^{1/2} \tag{1}$$

Where,

$Z = (15\times Z_C) + (18\times Z_H) + (8\times Z_N) + (7\times Z_O) = 100$ is the total number of valance electrons, ρ is the density and M is the molecular weight of BNPM crystal. Explicitly dependent on $\hbar\omega_p$ are Penn gap and the Femi energy [13] given by

$$E_p = \frac{\hbar\omega_p}{(\varepsilon_\infty - 1)^{1/2}} \tag{2}$$

and

$$E_F = 0.2948(\hbar\omega_p)^{4/3} \tag{3}$$

The polarisability α is determined by the relation [15]

$$\alpha = \left[\frac{(\hbar\omega_p)^2 S_0}{(\hbar\omega_p)^2 S_0 + 3E_p{}^2}\right] \times \frac{M}{\rho} \times 0.396\times 10^{-24} cm^3 \tag{4}$$

$$\text{Where} \quad S_0 = 1 - \left[\frac{E_p}{4E_F}\right] + \frac{1}{3}\left[\frac{E_p}{4E_F}\right]^2 \tag{5}$$

The value of α so obtained from the equation agrees well with that of Claussious-Mossotti equation as given by

$$\alpha = \frac{3M}{4\pi N_a \rho}\left(\frac{\varepsilon_\infty - 1}{\varepsilon_\infty + 2}\right) \quad (6)$$

All these calculated data for the grown crystal are presented in Table 1.

Table 1. Theoretical data on BNPM crystal.

Parameters	Values
Plasma energy (eV)	17.2200
Penn gap (eV)	0.4502
Fermi energy (eV)	13.1090
Polarisability (cm^3)	
Penn analysis	1.1052×10^{-22}
Clausious-Mossotti	1.1069×10^{-22}

4.3. Optical absorption analysis

The absorption spectrum of BNPM is shown in Fig. 3. There are three absorption peaks at 213, 229 and 317 nm may be due to electronic excitation of NO_2 group in p-nitrophenol [16,17] or colour of the material absorbing in and beyond the visible region [18]. At the longer wavelength side, the crystal is transparent upto 1200 nm. The lower cut-off wavelength of BNPM is found to be 462 nm. Thus the absence of absorption in the entire visible region between 462-800 nm shows that this crystal could be used for optical window applications [19].

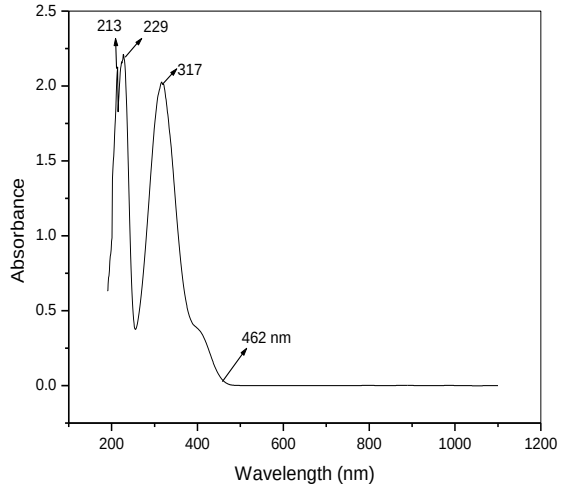

Fig. 3. UV-Vis spectrum of BNPM.

4.4. Micro hardness studies

Micro hardness test is one of the best methods for understanding the mechanical properties of the materials. The hardness of a material is defined as the resistance it offers to the motion of dislocations, deformation or damage under an applied stress [20]. The hardness and strength of the materials depends on dislocation movement of the material. Generally, the apparent hardness of the material varies with applied load. In order to investigate and compare the local deformation properties of BNPM crystals, micro hardness experiments have been performed on the prominent growth facets. Indentations were made on BNPM crystals for applied loads ranging from 25 gm to 100 gm. The static indentations were made at room temperature with a constant indentation time of 10s for all indentations. The average length of the indented impressions was used to calculate the hardness value. The Vicker's hardness was determined from the formula,

$$H_V = \frac{1.8544\ P}{d^2}\ \ kg/mm^2 \quad (7)$$

Where H_v is the Vicker's hardness number, P is the applied load in kg and d is the diagonal length of the indented impression in mm. Fig. 4a shows the variation of H_v as a function of applied load ranging from 25g to 100 g on the BNPM crystal. It is clear that microhardness increases with increase of load which reveals that the crystal exhibits reverse indentation size effect (RISE) [21] Meyar's law relates the size of indentation and load as [22]

$$P = k_1 d^n \quad (8)$$

where k_1 is a material constant and n is the Meyer's index.

$$\log P = \log k_1 + n \log d \quad (9)$$

The plot of log P against log d is shown in Fig. 4b is a straight line which is in good agreement with Meyer's law. Work hardening coefficient 'n' can be determined from the slope of the graph and it is found to 3.711. According to Onitsch [23] and Hanneman [24], value of n lies in between 1 – 1.6 for moderately hard materials and it is greater than 1.6 for the soft materials. Since work hardening coefficient 'n' is found to be 3.711, it is clear that BNPM belongs to soft material category.

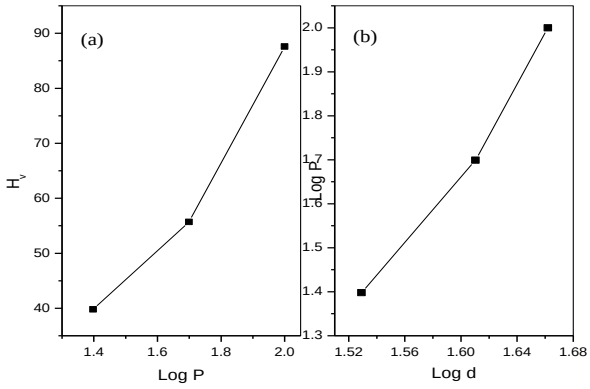

Fig. 4. Variation of Vickers hardness with load.

The value of materials constant (k_1) can be obtained from the plot of d^n versus p and it is shown in Fig. 5. The slope of straight line gives the value of materials constant (k_1). The resistance pressure of the crystalline material is a minimum load indentation (W) below which there is no plastic deformation [25]. Load dependence of hardness can be explained by Hays-Kendall law [26] as

$$P\text{-}W = k_2 d^2 \quad (10)$$

where k_2 is an another constant and (P-W) is the effective indentation test load considered in microhardness calculation. Plot between P versus d^2 shown in Fig. 5 which is a straight line. From these, the value of W which is the material resistance to the initiation of plastic flow can be estimated from intercept along the load axis and calculated to be 19.2g.

The elastic stiffness constant is calculated using Wooster's empirical formula [27] and it is represented by

$$C_{11} = H_v^{7/4} \quad (11)$$

which gives an idea about the tightness of bonding between the neighboring atoms and listed in Table 2.

Table 2. Calculated elastic stiffness values of BNPM.

Load *P/g*	C_{11}/Pa
25	1.95×10^{14}
50	3.52×10^{14}
100	7.77×10^{14}

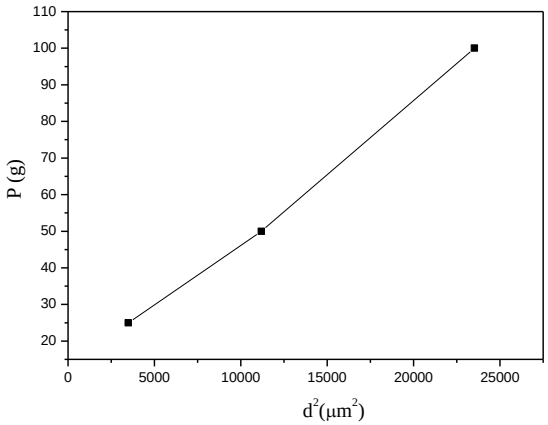

Fig. 5. Plot of d^n Vs p for BNPM.

4.5. Dielectric studies

The study of dielectric constant and dielectric loss factor as a function of temperature and frequencies are important for the design of microelectronic equipments. Fig. 6 and 7 shows the plot of temperature dependent dielectric constant and dielectric loss as a function of frequency. The dielectric constant of the sample is calculated for varying frequencies from 50Hz to 5 MHz under different temperatures ranging from 313 to 373 K by using the following relation

$$\varepsilon' = \frac{Cd}{\varepsilon_0 A} \quad (12)$$

$$\varepsilon'' = \varepsilon' \tan\delta \quad (13)$$

where C is the capacitance, d is the thickness of the sample and A is the area of the sample, ε_0 is the absolute permittivity of the free space.

The dielectric constant value is higher at lower frequencies for all temperatures and this is due to presence of space charge polarization [28]. It is seen from the Fig. 6 that as temperature increases, the value of dielectric constant also increases to a considerable value. The exchange of the charge carriers in the lattice sites is thermally activated by an increase in the temperature resulting increase in dielectric constant [29]. The value of dielectric constant decreases with increase of frequencies up to 100 KHz. For higher frequencies, the value of dielectric constant increases and then decreasing. It is seen from the Fig. 7 that dielectric loss values sharply decreases with increase in frequencies. The increase in losses at low frequencies is associated with the polarization of the trapped charge carriers i.e the dipole molecules cannot orient themselves in the lower temperature region. Due to thermal expansion, as the temperature increases, the orientation of dipoles is facilitated and this increases the dielectric constant [30]. With increase in frequency, polarization decreases and becomes very less at higher frequencies. This behavior is seen from the upward trend in the slopes of the dielectric constant and loss around 100KHz. This trend is not observed for lower frequencies and leads to dielectric relaxation at higher frequencies.

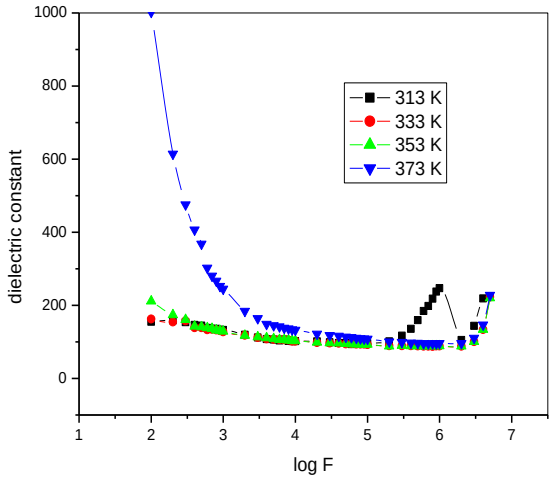

Fig. 6. Variation of dielectric constant with frequency for various temperatures.

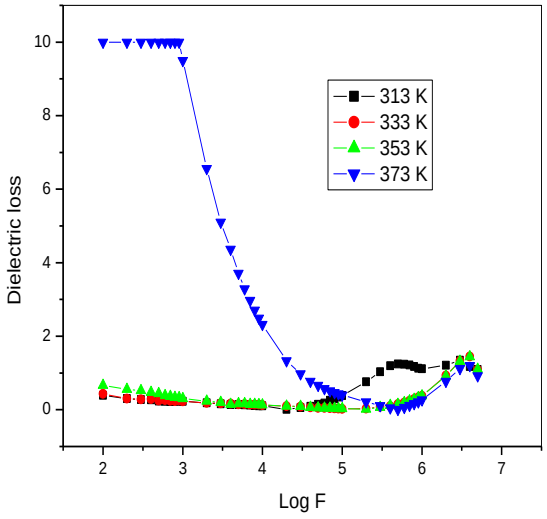

Fig. 7. Variation of dielectric loss with frequency for various temperatures.

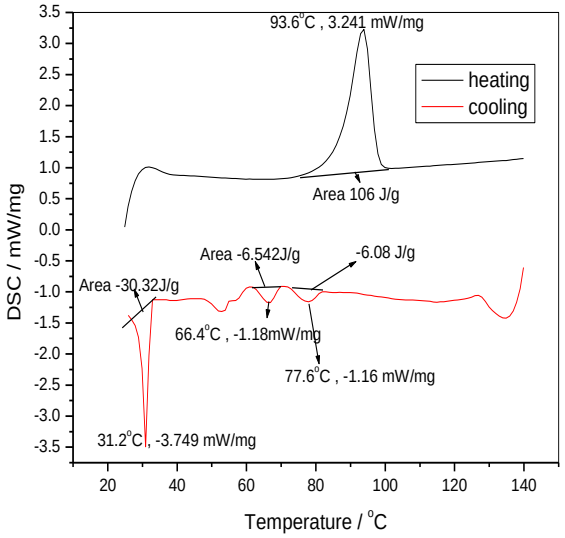

Fig. 8. DSC traces of BNPM.

4.6. Phase transition

Fig. 8 shows the DSC traces of BNPM. Differential scanning calorimetry measurements indicate clearly the occurrence of phase transition of the first order at approximately 366 and 304 K for heating and cooling respectively which is accompanied by a big thermal effect of 106 J/g. The peak at 366 K is due to the water of crystallization of BNPM. Similarly endothermic peaks can be associated with three stages of decomposition. The peak at 77.6°C may be due to crystallization of hydroxyl or nitro groups and the peak at 66.4°C may be due to crystallization of water molecules. At 31.2°C, the crystallization of BNPM would have occurred. From the heat flow value at the temperatures (ie) -6.08J/g at 77.8°C and -6.542J/g at 66.4°C, it is concluded that these may be due to solid state transition that has occurred in the crystallization of nitro and hydroxyl groups whereas at 31.2°C, the heat flow is found to be -30.32 J/g accounts for the crystallization of BNPM. The first stage of decomposition is the elimination of water molecule. The second stage of decomposition is accompanied by an elimination of two para nitrophenol molecules from BNPM. The third stage of thermal decomposition is the elimination of melamine which is usually occurs at ~ 500-600°C. In the present study, it is not the objective to find out the decomposition temperature of the final compound. The thermal stability of para nitrophenol and melamine is naturally higher since it has strong intermolecular hydrogen bonding which is expected to be present in these structures because of water of crystallization. Solid state transition that we have discussed may be due to either breaking or formation of hydrogen bonds during melting or crystallization as observed in endo or exothermic peaks.

4.7. SHG studies

Second harmonic generation test was performed to find the NLO property of the grown crystal by using Kurtz-Perry technique [31]. The crystals were grounded into powder and densely pakced in between two glass slides. Nd:YAG laser using the first harmonics output of 1064 nm with pulse width of 8 ns and repletion rate 10 Hz was passed through the sample. No detectable signal was observed thus the existence of symmetry center was confirmed. For centrosymmetric crystals second harmonic light should not be observed [32].

5. Conclusion

Co-crystallization of melamine and p-nitrophenol results in new organic crystalline product - bis (4-nitrophenol)-2,4,6-triamino 1,3,5- triazine monohydrate (BNPM). X-ray powder diffraction analysis confirms that BNPM crystallizes in triclinic system with centrosymmetric space group P-1. Some electronic parameters like plasma energy, Penn gap, Fermi energy and electronic polarizability of BNPM have been calculated. From the mechanical measurements, it was observed that the hardness increases with increase of load. Work hardening coefficient was found to be 3.711 and hence the material comes under soft category. The value of elastic stiffness constant (C_{11}) gives the strength of the bonds between the neighboring ions. Dielectric studies show that both dielectric constant and dielectric loss are less at high frequencies. DSC measurements on powder sample indicate the phase transition point at 366 and 306 K for heating and cooling respectively. No detectable signal was observed during second harmonic generation test.

References

[1] H. A. Cook, C. W. Klampfl, W. Buchberger, Electrophoresis, **26**, 1576 (2005).
[2] M. Drozd, M. K. Marchewka, J. Mol. Struc. (THEOCHEM), **716**, 175 (2005).
[3] J. Zieba-Palus, J. Mol. Struc. **327**, 511 (1999).
[4] Y. L. Wang, A. M. Mebel, C. J. Wu, Y. T. Chen, C. E. Lin, J. C. Jiang, J. Chem. Soc., Faraday Trans. **93**, 3445 (1997).
[5] R. J. Meier, A. Tiller, S. A. M. Vanhommerig, "J. Phys. Chem. **99**, 5457 (1995).
[6] W. J. Jones, W. J. Orville-Thomas, Trans. Faraday Soc. **55**, 193 (1959).
[7] P. J. Larkin, M. P. Makowski, L. A. Food, N. B. Colthoup, Vib Spectrosc. **17**, 53 (1998).
[8] R. J. Meier, J. R. Maple, M. J. Hwang, A. T. Hagler, J. Phys. Chem. **99**, 5445 (1995).
[9] J. R. Schneider, B. Schrader, J. Mol. Struct. **29**, 1 (1975).
[10] P. J. Larkin, M. P. Makowski, N. B. Colthoup, Spectrochim. Acta A, **55**, 1011 (1999).
[11] N. Kanagathara, G. Chakkaravarthi, M. K. Marchewka, S. Gunasekaran, G. Anbalagan, Acta Cryst. E **68**, o2286 (2012).
[12] N. Kanagathara, M. K. Marchewka, M. Drozd, N. G. Renganathan, S. Gunasekaran, G. Anbalagan, J. Mol. Struc. **1049**, 345 (2013).
[13] N. M. Ravindra, R. P. Bharadwaj, K. Sunil Kumar, V. K. Srivastava, Infrared Phys. **21**, 369 (1981).
[14] V. Kumar, B. S. R. Sastry, J. Phys. Chem. Solids, **66**, 99 (2005).
[15] N. M. Ravindra, V. K. Srivastava, Infrared Phys. **20**, 67 (1980).
[16] K. Kirupavathi, K. Selvaraju, S. Kumararaman, Spectrochimica Acta A, **71**, 1 (2008).
[17] G. Madhurambal, B. Ravindran, M. Mariappan, S. C. Mojumdar, J. Therm. Anal. Calorim, **100**, 811 (2010).
[18] M. Jose, B. Sridhar, G. Bhagavannarayana, K. Suganthi, R. Uthrakumar, C. Justin Raj, D. Tamilvendhan, S. Jerome Das, "J. Cryst. Growth. **312**, 793 (2010).
[19] N. Kanagathara, N. G. Renganathanm M. K. Marchewka, N. Sivakumar, K. Gayathri, P. Krishnan, S. Gunasekaran, G. Anbalagan, Spectrochim. Acta A, **101**, 112 (2013).
[20] B. W. Mott, Microindentation, Hardness testing, Butterworths, London, 206 (1956).
[21] P. Mythili, T. Kanagasekaran, Shailesh N. Sharma, R. Gopalakrishnan, J. Cryst. Growth **306**, 344 (2007).
[22] S. Dhanuskodi, T. C. Sabari Girisun, G. Bhagavannarayana, S. Uma, J. Philip, Mater. Chem. Phys. **126**, 463 (2011).
[23] E. M. Onitsch, Microscope, **95**, 12 (1950).
[24] M. Hanneman, Metall. Manch, **23**, 135 (1941).
[25] Vineeta Gupta, K. K. Bamzai, P. N. Kotru, B. M. Wanklyn, Mater. Chem. Phys, **89**, 64 (2005).
[26] C. Hays, E. G. Kendall, Metallography, **6**, 275 (1973).
[27] W. A. Wooster, Rep. Progr. Phys, **16**, 62 (1953).
[28] N. Ponpandian, P. Balaya, A. Narayanasamy, J. Phys. Condens. Matter. **14**, 3221 (2002).
[29] R. Balarew, J. Dushlew, Solid State Chem, **55**, 1 (1984).
[30] Vikram S Yadav, Devendra K Sahu, Yashpal Singh, D. C. Dhubkarya, Proceedings of the International MultiConference of Engineers and Computer Scientists **111**, 2010.
[31] S. K. Kurtz, T. T. Perry, J. Appl. Phys. **39**, 3798 (1968).
[32] V. G. Dmitrev, G. G. Gurzadyan, D. N. Nikogosyan, Handbook of Nonlinear Optical Crystals, Second Ed. Springer, 1997.

*Corresponding author: anbu24663@yahoo.co.in